applied sciences

MDPI

Article

Real-Time Mitigation of the Mobility Effect for IEEE 802.15.4g SUN MR-OFDM

Huy Nguyen , Nam Tuan Le , Nguyen Cong Hoan and Yeong Min Jang *

Department of Electronics Engineering, Kookmin University, Seoul 02707, Korea
* Correspondence: yjang@kookmin.ac.kr; Tel.: +82-2-910-5068

Received: 27 June 2019; Accepted: 8 August 2019; Published: 11 August 2019

Abstract: In order to develop wireless sensor networks, which are defined by the IEEE 802.15.4 specification, researchers are considering low-power wide-area networks (LPWAN) due to their advantages of being long range, low power, low cost, and highly mobile. The issue of mobility is covered in the IEEE 802.15.4g standard for supporting a smart utility network (SUN), which is mainly controlled by orthogonal frequency-division multiplexing (OFDM) modulation. In a high mobility scenario, inter-carrier interference is a primary factor in reducing the performance of OFDM transmissions due to the destruction of the subcarrier component's orthogonality. This paper analyzes the mobility effect in multi-rate multi-regional orthogonal frequency-division multiplexing (MR-OFDM) for low-power wide-area networks in general, and the SUN MR-OFDM system in particular. As mentioned in standard 802.15.4 2015, IEEE 802.15.4g MR-OFDM is one of the low-power wide-area (LPWA) technologies in which energy optimization problems are of first priority. We are especially interested in simple technologies that provide high efficiency. Therefore, we propose a highly adaptive method that uses the cyclic prefix to mitigate the mobility effect in real time. At a symbol frames interval of 120 us, the Doppler shift effect from the mobility of the MR-OFDM system adapted smoothly. This is not the best method to mitigate Doppler shift but it is a simple method that suits the LPWA network. The proposed scheme clearly simulated the mobility of the MR-OFDM system, and had the advantage of using a cyclic-prefix with a bit error rate performance through Additive White Gaussian Noise (AWGN) and the Rician channel of Matlab.

Keywords: MR-OFDM; SUN OFDM; mobility effect; carrier frequency offset; CFO; FCFO; fractional carrier frequency offset; doppler

1. Introduction

Low-power wide-area networks are attracting the attention of researchers worldwide because of their ability to connect low-power devices over large geographical areas. In the vision for the internet of things (IoT), LPWA technologies are seen as complementary and alternative technologies that support the conventional cellular and short-range wireless technologies for smart cities and machine-to-machine applications [1]. LPWA technology provides unique feature sets, including long-range, low-cost scalability, and low-power devices. The communication technology solution based on IEEE 802.15.4, which supports the mesh networking topology, has limitations in its communication range and data rate. Considering these problems, the IEEE 802.15.4g smart utility networks (SUNs) standard was proposed with a long communication range of several hundred meters and a data rate of 800 kbps. SUNs can also support a reliable mesh-routing protocol, which is expected to be a promising solution for mesh sensor networks.

The IEEE 802.15.4g SUN [2] is an amendment to the IEEE 802.15.4 standard [3], which has been processed to offer a global standard that facilitates large-scale process control applications, such as smart-grid networks. Three optional physical layers (hereinafter PHYs) have been proposed for SUN devices: multi-rate multi-regional frequency shift key (MR-FSK), multi-rate multi-regional orthogonal frequency shift key (MR-OFSK), and multi-rate multi-regional offset quadrature phase shift key (MR-O-QPSK). MR-FSK offers a good modulation scheme with a constant envelop signal that increases the transmission power efficiency. The MR-O-QPSK (DSSS) PHY converts multi-mode systems to more cost-effective and simpler designs. The multi-regional orthogonal frequency-division multiplexing (OFDM) was designed to supply higher rates in the delay spread channels. With the three PHYs, the MR-OFDM provides parameters to deal with the main standard scopes defined in the IEEE project authorization request, which is as follows [4]:

- Operation in the license-exempt frequency bands, such as 700 MHz to 1 GHz and in the 2.4-GHz band;
- Application mainly to outdoor communications;
- Data rate of IEEE 802.15.4 SUN to be at least 40 kbps and not greater than 1 Mbps;
- Mechanisms to coexist with other systems in the same bands, such as the IEEE 802.11 standard, IEEE 802.15 standard, and 802.16 standard.

The OFDM system is a special form of frequency-division multiplexing that divides the high rate stream into lower date streams called sub-streams, and simultaneously transmits all sub-streams through orthogonal subcarriers. In OFDM systems, the cyclic-prefix (CP) is added as the guard interval to combat inter-symbol interference (ISI), which seriously affects high rate systems due to multipath fading. Furthermore, the cyclic-prefix interval does not carry a signal, and it can reduce the system performance. Therefore, the length of the CP must be carefully chosen to balance between ISI reduction and effective performance. The principle disadvantage of OFDM is its sensitivity to frequency offsets caused by the Doppler shift and the asynchronous frequency of the local oscillators (LOs), which are also known as carrier frequency offsets (CFO). A CFO is a non-ideality in the baseband system design, which occurs when the LO signal in the receiver does not match the carrier signal in the transmitter. This phenomenon can occur in two cases: (i) frequency mismatch in the transceiver oscillators, and (ii) the Doppler effect as the transmitter and the receiver move relative to each other. When the CFO becomes present in the OFDM system, there is a frequency shift in the receiver's signal, which leads to non-orthogonality among the subcarriers. This can result in inter-carrier interference (ICI). The CFO includes two parts: integer frequency offset (IFO) and fractional frequency offset (FFO). IFO causes a circular shift of the subcarriers on the receiver side, which causes a significant degradation in the bit error rate (BER) performance. However, it does not destroy the orthogonality among the subcarrier frequency components; therefore, ICI does not appear. The presence of FFO will destroy the orthogonality among the subcarriers [5].

LPWA technologies offer some solutions for low-cost, long-range connectivity, and low-power operations for the IoT system. They allow IoT devices to operate stably up to 10 years on a single battery charge. Therefore, these technologies are ideal for smart cities, tracking and tracing, metering, and smart agriculture applications. LPWA technologies and IEEE 802.15.4 were applied with limited mobility; however, in some cases, we have needed to use LPWA technologies with a high mobility channel. With high mobility, IEEE 802.15.4g SUN MR-OFDM will be affected by CFO, especially the Doppler shift. In [6,7], the authors focused on the IFO estimation for IEEE 802.15.4g MR-OFDM, which ignored the effect and estimation of FFO. It uses only the preamble part to estimate and compensate the IFO in the entitled Physical Protocol Data Unit (PPDU) packet. Although FFO is very important, it causes non-orthogonality between subcarriers. In a mobility channel, the effects of CFO on the system vary in the time domain; therefore, we need the technical estimate and the compensated CFO in real time to combat the impact of the CFO on the system performance. In this paper, we analyze the impact of the Doppler shift on the IEEE 802.15.4g SUN MR-OFDM with high mobility between the transmitter and the receiver. In addition, we propose a novel method for the estimation and compensation of CFO in real time in the IEEE 802.15.4g SUN MR-OFDM. By using CP, which is the available part (cyclic-prefix part) in the MR-OFDM symbol frame, we can use it to estimate the CFO value without changing the architecture of symbol frames. In this way, the data rate of the system is not changed.

The remainder of this paper consists of four sections. Section 2 describes the analysis of the Doppler effect in the MR-OFDM system. Section 3 provides an overview of the IEEE 802.15.4g specifications and includes the related studies on MR-OFDM compensation. In Section 4, we describe our contributions, that is, the effects analysis of the CFO on the MR-OFDM principle and of the proposed scheme on the OFDM compensation. Section 5 explains the performance evaluation with different configuration scenarios. Then, the final section concludes the paper.

2. Analysis of the Doppler Shift

In this paper, we consider smart meter applications of the MR-OFDM transceivers that are located in harsh or radioactive areas where energy is very important for communication devices. To measure and collect environmental parameters in such areas, we cannot use conventional technologies; instead, we need to use LPWA technology. There are a number of reasons for this. First, in extremely harsh environments, we cannot usually change the battery or use electricity networks to provide energy for sensors. In such situations, LPWA technology is advantageous. Second, when the sensors are located in a large field, we need technologies that can transmit data long distances. Third, we use unmanned aerial vehicles (UAV) that fly over these regions to collect data daily. When a large amount of data is required in one day, we need a high-bit-rate digital communication link that consumes low power. Then, we focus on MR-OFDM out of the three SUN PHYs. This scenario is represented in Figure 1.

The high speed of the receiver mobility leads to a Doppler shift in the system. The Doppler shift causes the CFO to affect the system performance. A Doppler shift occurs when there is a movement between the receiver and the transmitter:

$$f_d(t) = f_c.\frac{v(t)}{c}\cos\alpha(t) = f_{\max}\cos\alpha(t) \tag{1}$$

Here, f_c is the center carrier frequency; $v(t)$ is the velocity of the receiver; c is the speed of light; and α is the angle of arrival, which is the angle between the arriving wave and the direction of motion, as show in Figure 1.

When the receiver moves with the constant velocity v, the changes in the angle of arrival are given as follows [8]:

$$\cos\alpha(t) = \frac{D_s/2 - v(t).t}{\sqrt{d^2 + (D_s/2 - v(t).t)^2 + \Delta h^2}} \text{ with } 0 \le t \le D_s/v(t) \tag{2}$$

$$\cos\alpha(t) = \frac{-1.5D_s + v(t).t}{\sqrt{d^2 + (-1.5D_s + v(t).t)^2 + \Delta h^2}} \text{ with } D_s/v(t) < t \le 2D_s/v(t) \tag{3}$$

$$\text{With } \cos\alpha(t) = \cos\alpha(t \bmod (2D_s/v(t))),\ t > 2D_s/v(t) \tag{4}$$

Here, D_s is the distance between two of the transmitters; d is the minimum distance between the transmitter and the moving direction (as in Figure 1); and Δh is the height difference between the receiver and the transmitter. According to [9], the CFO ε is the ratio of the offset frequency to the subcarrier spacing Δf. As mentioned above, the CFO causes a frequency shift at each subcarrier of the receiver. This is presented as follows:

$$\varepsilon = \frac{f_{offset}}{\Delta f} \tag{5}$$

At the velocity of 75 m/s, the maximum Doppler value is 600 Hz because the maximum CFO value is 0.0576, and Δf is 10,417 Hz. This shows that the FFO causes ICI, which causes a non-orthogonality between the subcarriers. This reduces the system performance. In this paper, we propose a novel scheme that can estimate and compensate for the Doppler effect in real time by using the CP part, which was added to the OFDM symbol to combat ISI.

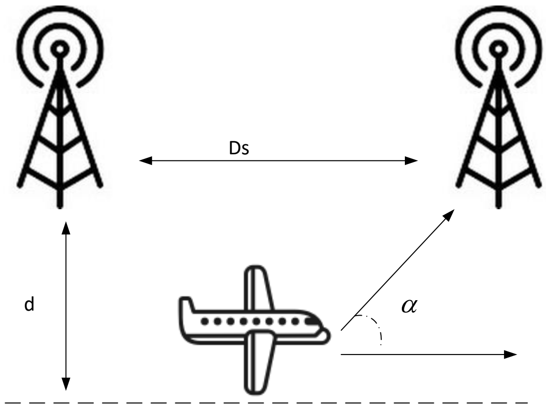

Figure 1. Scenario of a practical system.

3. Related Works

3.1. Overview of IEEE 802.15.4g MR-OFDM

In the global industry, the IEEE 802 is considered to be one of the most demanding standardization organizations over the last decade. In 2012, the IEEE 802.15.4g task group standardized the PHY amendment for the IEEE 802.15.4 specifications by supporting the SUN technique to create a new direction for the LPWA sensor network. The IEEE 802.15.4g PHYs SUN specification defined two configuration modes: low data rate and high data rate. When considering the applications, the IEEE 802.15.4g PHYs included multi-rate MR-FSK, multi-rate MR-OFDM, and MR-O-QPSK. The configuration summaries of IEEE 802.15.4g SUN OFDM PHY are shown in Table 1. This mode can support a range of data rates from 50 kbps to 800 kbps with the 10.416 kHz constant of the subcarrier spacing with four configuration options. Every option mode is differentiated by the number of active tones, the channel bandwidth, the sensitivity level, and the data rates. The total signal bandwidth for each mode ranges from 1.2 MHz to 200 kHz depending on the number of active tones. All devices are required to support the particular hardware options, which are supported by the BPSK, the QPSK modulation, and the 16-QAM option. The PHY frame structure was modified with forward error coding information and a header up to a 1500-octet frame length from the start frame delimiter. The preamble includes the short training field (STF) for synchronization and the long training field (LTF) for the signal-to-noise ratio (SNR) estimation. In each STF symbol, there are five 16-length symbols. One LTF defines two symbols, S1 and S2, with a double CP for N samples.

The MR-OFDM was formatted as shown in Figure 2. Based on IEEE 802.15.4g, the MR-OFDM includes four modes; each mode is determined by the number of active tones. This standard supports the following baseline DFT sizes: 16, 32, 64, and 128. Table 1 shows more details about the four modes of the MR-OFDM. The MR-OFDM symbol rate was 8-1/3 ksymbol/s; each symbol corresponds to 120 us. This symbol period includes the CP (24 us) and a base symbol part (96 us). The synchronization header (hereinafter SHR) includes the STF and the LTF. It is used as a preamble for detecting the start of the frame. After SHR, the PHY header carries the frame configuration, code rate, frame length, scrambler, and other information fields. The packet service data unit is the payload of the packet that carries the useful data. According to the standards, the STF field is divided into four OFDM symbols; in the fourth symbol, the last half was negated in the time domain, which is important for defining the synchronization algorithm. In addition, a quarter-duration of CP is added to each symbol. The LTF field is described by two OFDM symbols. A half-symbol CP is inserted into two consecutive copies of the LTF symbol; this prefix is used to estimate IFO.

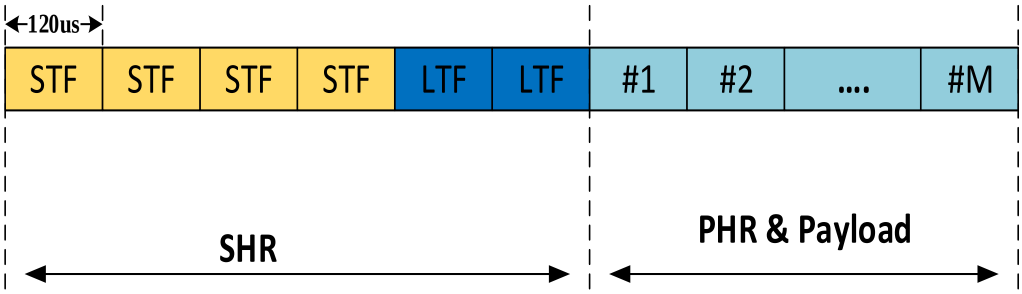

Figure 2. Structure of a packet.

Table 1. Data rates for IEEE 802.15.4g SUN MR-OFDM [10].

Parameter	Option 1	Option 2	Option 3	Option 4
Nominal bandwidth (kHz)	1094	552	281	156
Channel spacing (kHz)	1200	800	400	200
DFT size	128	64	32	16
Active tones	104	52	26	14
#Pilot tones	8	4	2	2
#Data tones	96	48	24	12
Subcarrier	10.416	10.416	10.416	10.416
Data rate (kbps)	100–800	50–800	50–600	50–300
Power sensitivity (dBm), PER < 10%	−103	−105	−105	−105

3.2. Overview of CFO Estimation Technologies

Due to the effect of CFO on the channel estimation, CFO estimation is a very important factor in the OFDM systems design and optimization. Many researchers have focused on finding the CFO estimation methods. The CFO can be estimated in two ways: the time-domain estimation techniques (or pre-FFT synchronization) and frequency-domain estimation techniques (or post-FFT synchronization). Pre-FFT synchronization is the estimation performed before the OFDM demodulation (FFT processing). The advantage of the pre-FFT approach is that it requires less estimation time and less computing power because the FFT process is not needed. Pre-FFT synchronization can be divided into two categories: data-aided (DA) and non-data-aided (NDA) [11,12]. The DA methods [13,14] insert a known OFDM training symbol into the start of every OFDM packet for the purpose of FFO estimation. The disadvantage of these approaches is that they reduce the data transmission efficiency because the training symbols need to be inserted in the OFDM packet in exchange for a CFO estimation range wider than the NDA algorithms [−1, +1] [15]. The NDA methods use the CP part to estimate the fractional CFO [16,17]. They take advantage of the correlation of the CP and the corresponding OFDM symbol part to estimate the FFO. However, this method can only estimate the CFO in the range of [−0.5, +0.5] [18], but it does not need additional OFDM training symbols, which improves the data transmission efficiency. Post-FFT synchronization is the estimation method performed after the FFT processing. This method takes advantage of the correlation between the received pilot subcarriers and a shifted version of the known pilot subcarriers [19] to estimate the CFO. Depending on the spacing among pilot subcarriers, the CFO range up to multiple integers can be estimated. Usually, post-FFT synchronization is employed for the IFO left estimation after pre-FFT synchronization. We chose the appropriate approach depending on the specifications and the system requirements.

3.3. Research on MR-OFDM Compensation

The MR-OFDM-compliant research from [20] proposed a complementary–metal–oxide–semiconductor architecture for the IEEE 802.15.4g SUN receiver and transceiver with a zero-IF architecture, low-frequency noise, and circuit-based dc offset control for energy efficiency in smart grids. The measured sensitivity for the data rate of 100 kbps was −103 dBm with a PER of 1%. However, the compensation for the mobile scenario topology was not considered. The SNR estimation for IEEE

802.15.4g MR-OFDM from [21] used the preamble signal over the frequency selective fading channels. From the structure of the IEEE 802.15.4 specification with the STF and the LTF, we calculated the estimate by using the preamble signal on which the inverse fast Fourier transform, the CP, and the Rayleigh fading were used.

In [6], the authors used STF, which was made by a pseudo noise sequence, to estimate the integer frequency offset, whereas [7] proposed algorithms that used the LTF in the preamble to estimate the IFO by using the LTF format in advance, as show in Figure 2. They estimated the CFO accurately for each packet. However, with the dynamic channel, the CFO can be changed in each OFDM symbol. The conventional algorithms that use the preamble part to estimate the CFO seem no longer suitable, especially with the environments that have fast change-over times. In this paper, we propose a scheme that can estimate and compensate for the CFO in real time for changing environments.

4. Adaptive Estimation and Compensation for the CFO Scheme

4.1. Effects of CFO to MR-OFDM

The OFDM technology is a common technique that has several advantages in regards to digital transmissions over frequency-selective fading channels. However, the principal weakness of OFDM is the sensitivity of frequency offsets because of motion-induced Doppler shifts and the LO frequency mismatch. In this paper, we assume that the system has been synchronized in time and in oscillator frequency. The OFDM signal of the baseband in the frequency domain is given as follows:

$$x[n] = \sum_{k=0}^{N-1} X[k].e^{j2\Pi k/N} \tag{6}$$

Here, $X[k]$ is the symbol transmitted by the k-th subcarrier.

As mentioned in Section 2, we focus on the fractional CFO, and the received baseband signal under the presence of an FFO of ε as follows:

$$y_l[n] = \frac{1}{N}\sum_{k=0}^{N-1} H_l[k]X_l[k]e^{j2\Pi(k+\varepsilon)/N} + z_l[n] \tag{7}$$

Here, N is the FFT size; l is the sequence number of the symbol in the packet; and z is the Gaussian noise.

The frequency domain of the received signal with an FFO of ε is as follows [17]:

$$Y_l = FFT\{y_l[n]\} = \sum_{n=0}^{N-1} y_l[n]e^{-j2\Pi kn/N} = (\sum_{n=0}^{N-1}\frac{1}{N}\sum_{m=0}^{M-1} H[m]X_l[m]e^{j2\Pi(m+\varepsilon)n/N} + z_l[n])e^{-j2\Pi kn/N} \tag{8}$$

$$\begin{aligned} Y_l[k] &= e^{j\Pi\varepsilon(N-1)/N}\left\{\frac{\sin(\Pi\varepsilon)}{N\sin(\Pi\varepsilon/N)}\right\}H_l[k]X_l[k] \\ &+ e^{j\Pi\varepsilon(N-1)/N}\sum_{m=0,m\neq k}^{N-1}\frac{\sin(\Pi(m-k+\varepsilon))}{N\sin(\Pi(m-k+\varepsilon)/N)}H[m]X_l[m]e^{j\Pi(m-k)(N-1)/N} + Z_l[k] \end{aligned} \tag{9}$$

$$Y_l[k] = e^{j\Pi\varepsilon(N-1)/N}\left\{\frac{\sin(\Pi\varepsilon)}{N\sin(\Pi\varepsilon/N)}\right\}H_l[k]X_l[k] + I_l[k] + Z_l[k] \tag{10}$$

$$I_l[k] = e^{j\Pi\varepsilon(N-1)/N}\sum_{m=0,m\neq k}^{N-1}\frac{\sin(\Pi(m-k+\varepsilon))}{N\sin(\Pi(m-k+\varepsilon)/N)}H[m]X_l[m]e^{j\Pi(m-k)(N-1)/N} \tag{11}$$

where $I_l[k]$ represents the ICI from other subcarriers to the k-th subcarrier with an FFO of ε.

As known, if the system has an FFO of $\varepsilon = 0$, the ICI value as shown in Equation (11) equals 0, which illustrates that the orthogonality of subcarriers was guaranteed. Orthogonality is very important with the OFDM system, as it causes a reduction in the system performance. The signal is distorted because of FFO with amplitude and phase distortions, shown in the first term of Equation (9).

4.2. Proposed Scheme

As mentioned in Section 3, estimating the CFO technique by using the CP has certain advantages, such as spending less time in estimation and using less computing power. The range of the CFO can be estimated as [−0.5, +0.5]. In this section, we take advantage of the CP technique for the CFO estimator in each OFDM symbol. CP is an important part of the OFDM symbol, which is the tail of the symbol copied to the top of the symbol for reducing ISI. We assume that the symbol synchronization is perfect, and the CFO of the ε value causes a phase rotation of $2\Pi n\varepsilon/N$ at the receiver side. If the channel equalizer is perfect, the channel effect of the OFDM symbol can be considered negligible. In this case, the phase difference between the CP part and the corresponding tail of the OFDM symbol is $2\Pi N\varepsilon/N = 2\Pi\varepsilon$ as follow:

$$y_l[n] = x_l[n]e^{\frac{2\Pi n\varepsilon}{N}} \text{ with } n = -N_{CP}, -N_{CP}+1, \ldots\ldots, -1 \tag{12}$$

$$y_l[n+N] = x_l[n]e^{\frac{2\Pi(n+N)\varepsilon}{N}} \text{ with } n = -N_{CP}, -N_{CP}+1, \ldots\ldots, -1 \tag{13}$$

Then, the CFO value can be detected by comparing the phase of the CP part with the phase of the corresponding tail of the OFDM symbol, which is defined as follows:

$$\widehat{\varepsilon} = \frac{1}{2\Pi}\arg\left\{y_l^*[n]y_l[n+N]\right\} \text{ with } n = -N_{CP}, -N_{CP}+1, \ldots\ldots, -1 \tag{14}$$

To reduce the effects of noise, the estimated value of the CFO is taken as the average of the total N_{CP} samples as follows:

$$\widehat{\varepsilon} = \frac{1}{2\Pi N_{CP}}\arg\left\{\sum_{n=-N_{CP}}^{-1} y_l^*[n]y_l[n+N]\right\} \text{ with } n = -N_{CP}, -N_{CP}+1, \ldots\ldots, -1 \tag{15}$$

If N_{CP} is the number of CP, and N is the DFT size, then the argument operation arg{} is $\tan^{-1}$ {} with the CFO estimate in the range [−0.5, +0.5].

The proposed scheme that uses CP to estimate and compensate for the CFO is shown in Figure 3. After the signal goes through the equalizer block, the signal is divided into two parts. First, the signal goes through the CFO estimation block using the CP technique. Second, the signal is given over to the CFO compensation block with input from the CFO estimation block. Figure 4 shown the constellation of the MR-OFDM with the CFO effect and after CFO compensation over the Gaussian channel. We can see that the system performance is improved after using the proposed scheme.

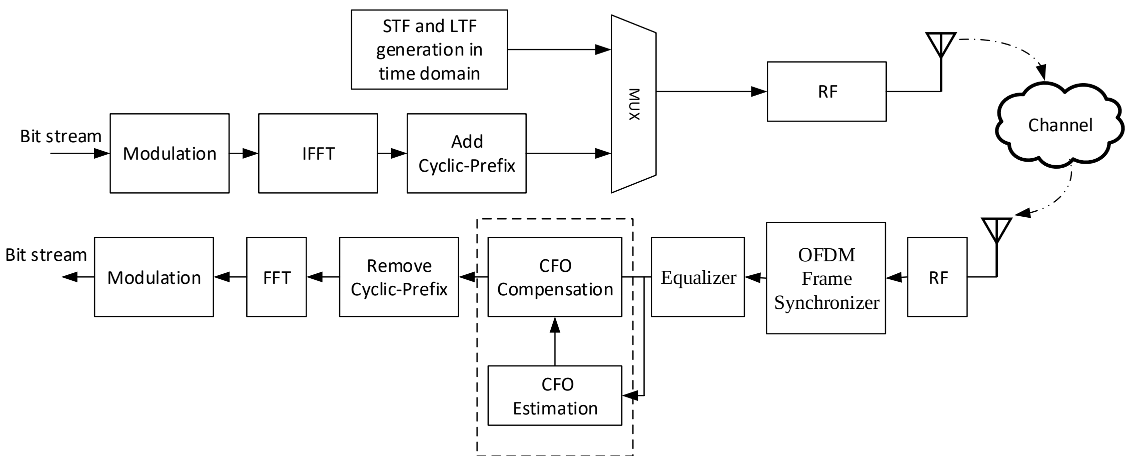

Figure 3. Block diagram of the architecture of the proposed scheme.

Figure 5 evaluates the CFO estimation effectiveness of the CP method using four options based on the mean-squared error algorism. From Equation (15), the estimated value of the CFO will be better if the DFT windows sizes are larger. Figure 5 shows that the estimated performance of Option 1 is the best because of the DFT size of 128, and the estimated performance of Option 4 is the lowest because of the DFT size of 16 at the same noise level.

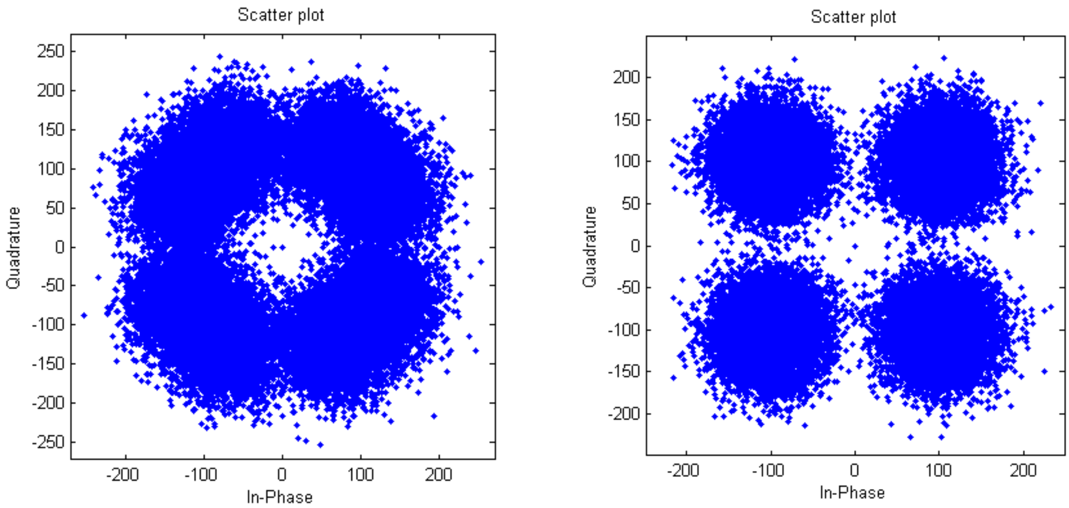

(**a**) (**b**)

Figure 4. (**a**) Constellation of the MR-OFDM with the CFO effect; (**b**) Constellation of the MR-OFDM after CFO compensation over the Gaussian channel.

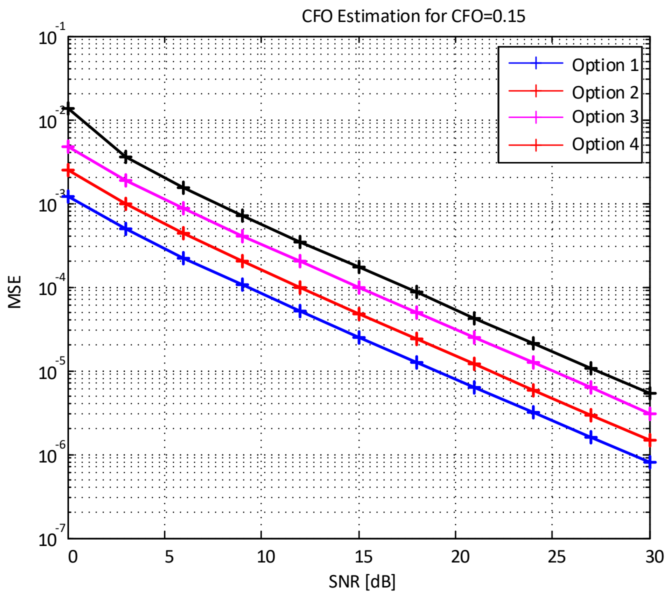

Figure 5. MSE of the cyclic prefix technique with four options.

5. Performance Evaluation

In this section, we use the CP method to estimate and compensate for the CFO in MR-OFDM; this simulation is based on the characteristic parameters shown in Table 2.

In this paper, we illuminate three speed cases, which can occur with this system. There are three popular cases concerning the velocity of UAV: constant, increased, and decreased. In the constant velocity case, we simulate the velocity of UAV of 75 m/s. In the decreased velocity scenario, we simulate the velocity of UAV decreasing from 75 m/s to 0 m/s with the acceleration of $a = -0.5$ m/s^2. With the increased velocity scenario, we simulate the velocity of UAV increasing from 0 m/s to 75 m/s with the acceleration of $a = 0.5$ m/s^2. After achieving 75 m/s, the UAV will move with the constant velocity of 75 m/s.

Table 2. Characteristic parameters for simulation.

Parameters	Values
Antenna height of the transmitter	6 m
Height of the unmanned aerial vehicle	10 m
Distance between the routes with the transmitter (d)	10 m
Velocity of the unmanned aerial vehicle (v)	75 m/s
MR-OFDM Option mode 1	$N_{FFT} = 128$, QPSK
Frequency	2.4 GHz
Channel	AWGN, Rician
Bit rate	773.809 kbps

Figures 6–8 represent the simulated CFO over time and the estimated CFO over time by using the CP algorism shown in Equation (15) with three cases. We can see that the CFO value and the Doppler shift are proportional. If the value of CFO changes during the transmission time, then we need a technique that can estimate the CFO in real time to compensate the CFO and then, increase the system performance. In our proposed scheme, the CP technique can exactly estimate the CFO value for every 120 us of the OFDM symbol frame. Therefore, the CP technique is suitable for the system when the shape of the estimated CFO value is the same as the shape of the practical CFO in real time. In addition, their values are the same and show the effectiveness of the proposed algorism in real time.

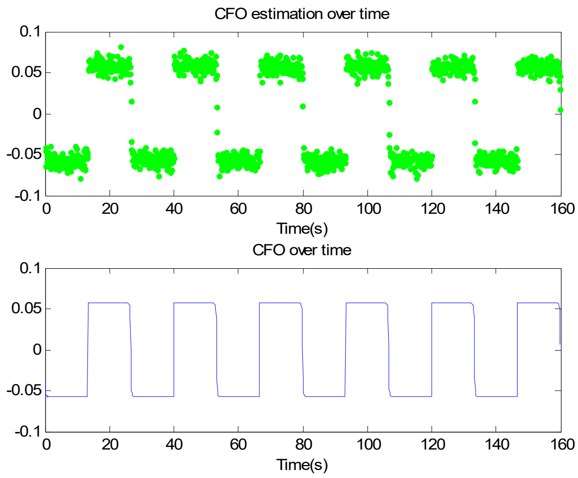

Figure 6. CFO estimation over time with a constant velocity (v = 75 m/s).

Figures 9–11 show the BER performance when the receiver moves at the three velocities over the Gaussian channel and the Rician channel with k = 10. The blue line represents the BER performance of the MR-OFDM without the CFO effect. The green line represents the BER performance of the MR-OFDM at the three velocities: constant, decreased and increased, and the red line shows the BER performance of the MR-OFDM system after the proposed scheme. A comparison between the blue line and the green line in the three cases shows the influence of the Doppler effect on the system performance. In addition, the red line and the blue line almost overlap in all three cases indicating that the proposed scheme can almost estimate and compensate for the Doppler shift in the Rician channel and the Gaussian channel. Because the proposed scheme can estimate the CFO in each OFDM symbol, then, in the future, we could apply this scheme for movements with random velocity changes in the transceiver.

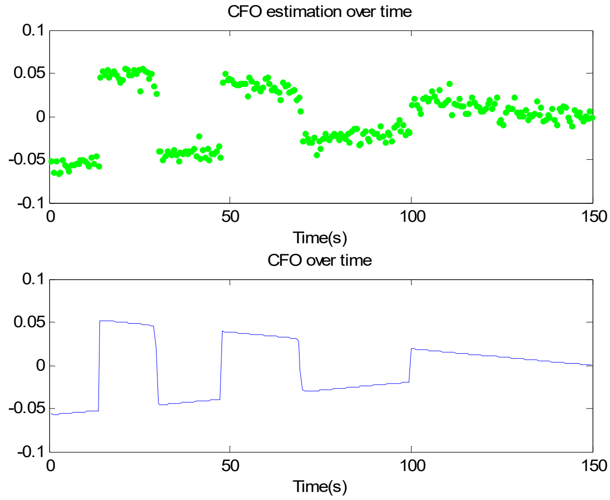

Figure 7. CFO estimation over time with the acceleration of $a = -0.5$ m/s^2.

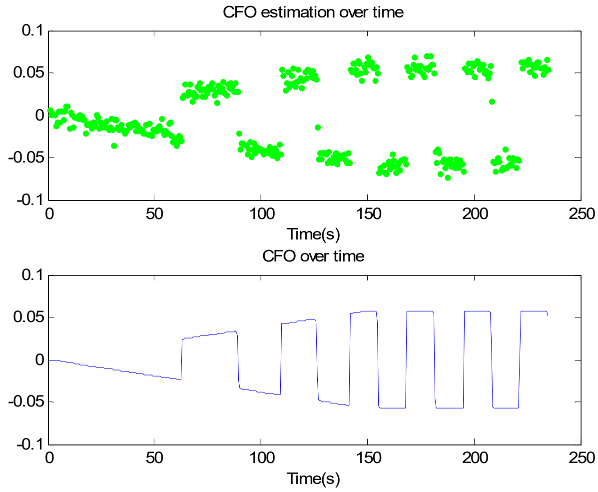

Figure 8. CFO estimation over time with the acceleration of $a = 0.5$ m/s^2.

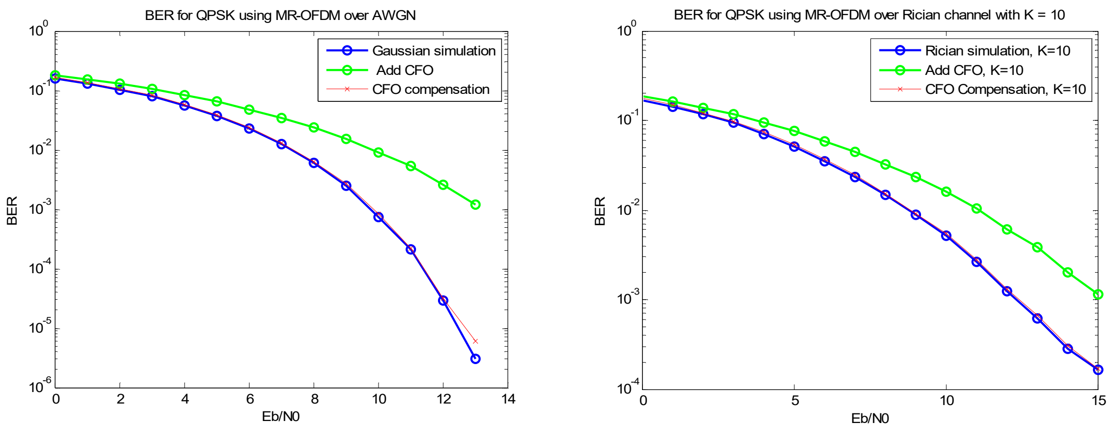

Figure 9. Simulation BER per Eb/N0 of MR-OFDM over the Gaussian and Rician channels with a constant velocity (v = 75 m/s).

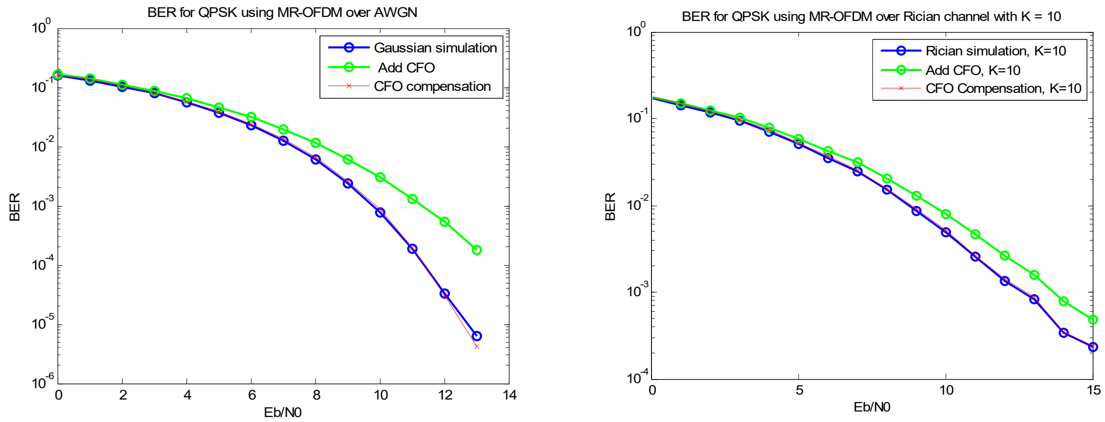

Figure 10. Simulation BER per Eb/N0 of MR-OFDM over the Gaussian and Rician channels with the acceleration of $a = -0.5$ m/s^2.

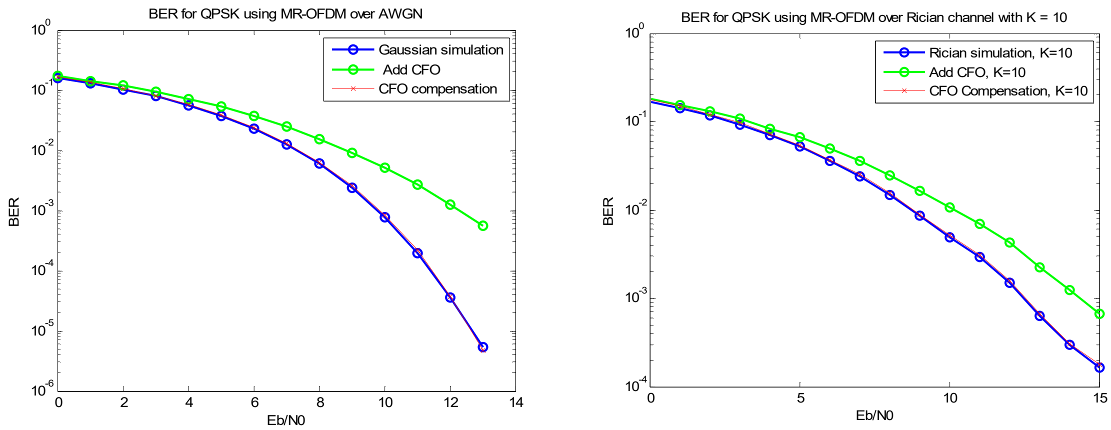

Figure 11. Simulation BER per Eb/N0 of MR-OFDM over the Gaussian and Rician channels with the acceleration of $a = 0.5$ m/s^2.

6. Conclusions

In this paper, we showed the effect of the Doppler on IEEE 802.15.4g SUN OFDM PHY with a high mobility application scenario. From the trajectory of the Doppler frequency with the velocity between Tx and Rx, we proposed a novel method to enhance the performance of the MR-OFDM signal. Our method takes advantage of the CP part to estimate and compensate for the fractional CFO. The performance of this method shows its effectiveness for the mobility of the IEEE 802.15.4g MR-OFDM system.

Author Contributions: All authors contributed to this paper: H.N. and N.T.L. proposed the idea and simulation methodology; H.N. optimized software, proposed and designed the proposed scheme, performed all experiments, and wrote paper; N.T.L. verified the experiment process and results, reviewed and edited the paper; and Y.M.J. supervised the work and provided funding support.

Funding: This research was supported by the MSIT (Ministry of Science and ICT), Korea, under the ITRC (Information Technology Research Center) support program (IITP-2018-0-01396) supervised by the IITP (Institute for Information & communications Technology Promotion).

Conflicts of Interest: The authors declare no conflict of interest.

References

1. Raza, U.; Kulkarni, P.; Sooriyabandara, M. Low power wide area networks: An overview. *IEEE Commun. Surv. Tutor.* **2017**, *19*, 855–873. [CrossRef]
2. IEEE. *Standard IEEE 802.15.4g 2012*; IEEE: Piscataway Township, NJ, USA, 2012.
3. IEEE. *Standard IEEE 802.15.4 2011*; IEEE: Piscataway Township, NJ, USA, 2011.

4. *IEEE std. 802.15.4g Project Authorization Request (PAR)*; Wireless Personal Area Network (WPAN) Working Group: Piscataway, NJ, USA, March 2012.
5. Liu, M.; Chen, J.; Li, B.; Li, J. Fractional frequency offset estimation for OFDM systems in non-cooperative communication. *China Commun.* **2016**, *13*, 65–71. [CrossRef]
6. Kim, B.; Choi, S. Integer frequency offset estimation for IEEE 802.15.4g SUN MR-OFDM PHY. In Proceedings of the 2011 5th International Conference on Signal Processing and Communication Systems (ICSPCS), Honolulu, HI, USA, 12–14 December 2011.
7. Alves-Tamagno, D.C.; de Lima, E.R.; Lopes, R.R. A low complexity ICFO estimator and compensator for IEEE 802.15.4g MR-OFDM. In Proceedings of the 2018 IEEE 29th Annual International Symposium on Personal, Indoor and Mobile Radio Communications (PIMRC), Bologna, Italy, 9–12 September 2018.
8. Liu, L.; Cheng, T.; Rongchen, S.; Houjin, C. A modified doppler frequency trajectory undergoing varying velocities in HSR communications. *China Commun.* **2016**, *13*, 17–21. [CrossRef]
9. Soo, C.Y.; Kim, J.; Yang, W.Y.; Chung, K.G. *MIMO-OFDM Wireless Communications with MATLAB*; Wiley-IEEE Press: Hoboken, NJ, USA, 2010.
10. IEEE. *Standard IEEE 802.15.4 2015*; IEEE: Piscataway Township, NJ, USA, 2015.
11. Al-Bassiouni, A.A.M.; Ismail, M.; Zhuang, W. An eigenvalue based carrier frequency offset estimator for OFDM systems. *IEEE Wirel. Commun. Lett.* **2013**, *2*, 475–478. [CrossRef]
12. Nishad, P.K.; Singh, P. Carrier frequency offset estimation in OFDM systems. In Proceedings of the 2013 IEEE Conference on Information & Communication Technologies, Thuckalay, India, 11–12 April 2013.
13. Anju, A.A. Estimation techniques for CFO. *Int. J. Recent Res. Asp.* **2016**, *3*, 122–126.
14. Raboh, M.S.A.; Zakaria, H.M.; Al Bassiouni, A.A.M.; El Bahy, M.M. Carrier Frequency Offset (CFO) Estimation Methods, a Comparative Study. Available online: http://www.bu.edu.eg/ (accessed on 23 February 2017).
15. Kevin, W.; Singh, J.; Faulkner, M. FPGA implementation of an OFDM WLAN synchronizer. In Proceedings of the DELTA 2004 Second IEEE International Workshop on Electronic Design, Test and Applications, Perth, Australia, 28–30 January 2004.
16. Qiao, Y.; Wang, Z.; Ji, Y. Blind frequency offset estimation based on cyclic prefix and virtual subcarriers in co-OFDM system. *Chin. Opt. Lett.* **2010**, *8*, 888–893. [CrossRef]
17. Abshir, A.G.; Abdullahi, M.M.; Samad, M.A. A comparative study of carrier frequency offset (CFO) estimation techniques for OFDM systems. *IOSR J. Electron. Commun. Eng.* **2014**, *9*, 1–6. [CrossRef]
18. Van de Beek, J.J.; Sandell, M.; Borjesson, P.O. ML estimation of timing and frequency offset in OFDM systems. *IEEE Trans. Signal Process.* **1997**, *45*, 1800–1805. [CrossRef]
19. Ren, G.; Chang, Y.; Zhang, H.; Zhang, H. An efficient frequency offset estimation method with a large range for wireless OFDM systems. *IEEE Trans. Veh. Technol.* **2007**, *56*, 1892–1895.
20. Lee, S.; Seo, Y.; Kim, B.; Choi, S.; Kim, C. An IEEE 802.15.4g sun compliant MR-OFDM RF CMOS transceiver for smart grid and CES. *IEEE Trans. Consum. Electron.* **2013**, *59*, 460–466. [CrossRef]
21. Aloui, A.; Rhouma, O.B.; Rebai, C. Preamble based SNR estimation for IEEE 802.15.4g MR-OFDM. In Proceedings of the 2018 25th IEEE International Conference on Electronics, Circuits and Systems (ICECS), Bordeaux, France, 9–12 December 2018.